ITC 4/52
Information Technology and Control
Vol. 52 / No. 4 / 2023
pp. 887-897
DOI 10.5755/j01.itc.52.4.34476

Apply Physical System Model and Computer Algorithm to Identify Osmanthus Fragrans Seed Vigor Based on Hyperspectral Imaging and Convolutional Neural Network

Received 2023/06/25 | Accepted after revision 2023/10/03

HOW TO CITE: Qiu, C., Ding, F., He, X., Wang, M. (2023). Apply Physical System Model and Computer Algorithm to Identify Osmanthus Fragrans Seed Vigor Based on Hyperspectral Imaging and Convolutional Neural Network. *Information Technology and Control*, 52(4), 887-897. https://doi.org/10.5755/j01.itc.52.4.34476

Apply Physical System Model and Computer Algorithm to Identify Osmanthus Fragrans Seed Vigor Based on Hyperspectral Imaging and Convolutional Neural Network

Caihua Qiu
Guangdong University of Science and Technology, 99 Xihu Road, Nancheng District, Dongguan Guangdong, China, 523083

Feng Ding, Xiu He, Mengbo Wang
Guangzhou Xinhua University, 248 Yanjianxi Road, Machong Town, Dongguan Guangdong, China, 523133

Corresponding author: dingfeng@xhsysu.edu.cn

Rapid identification of seed vitality plays key roles in the cultivation of the agricultural and forestry crops. This study discusses the use of compose a specular like technology, the computer algorithm and the feasibility of the physical system identification under different osmanthus seed vigor, in order to improve the ability to recognize. Two varieties of Osmanthus seeds (JinQiGui and RiXiangGui) were artificially aged and then hyperspectral data were collected. Multivariate scattering correction (MSC) and competitive adaptive reweighted sampling algorithm (CARS) were used for spectral preprocessing and feature wavelength selection, respectively. The extreme learning machine (ELM) and k-nearest neighbor (KNN) were used to establish the spectral discriminant model, and convolutional neural network was used in the computer image discriminant model. When MSC+CARS is combined with the above Discriminative model, nearly 100% recognition can be achieved with fewer bands. Compared with machine learning model, image-depth learning model can get higher model accuracy for different vigor JQG and RXG without complex preprocessing. These results indicate that hyperspectral imaging technology can effectively distinguish different vigor of Osmanthus fragrans seeds based on computer technology and physical system. Combining deep neural networks with image information is of great importance for research and development of portable high precision seed vitality spectral imagers.

KEYWORDS: Hyperspectral imaging, Osmanthus fragrans, Seed vgor, Discriminant model, Feature band selection.

1. Introduction

Seed vitality is the sum of seed germination rate, germination rate, seedling growth potential, plant stress resistance, and production potential, and is an important indicator for evaluating seed quality [4]. The seeds of high vigor can sprout rapidly or uniformly in the field to ensure the whole seedling and the field density of crops. It can also lay a good foundation for increasing production and at the same time have a strong resistance to field adversity. Therefore, selecting seeds with high vigor before sowing is of great significance to plant growth and yield increase.

Osmanthus fragrans, one of the ten famous traditional Chinese flowers [5], is an excellent ornamental and practical garden tree species that integrates greening, beautification, and fragrance. Osmanthus fragrans has important medicinal value. As a raw material, osmanthus tea is widely promoted, and it is also widely used in garden construction. Through artificial cultivation, natural hybridization and artificial selection, a rich variety of cultivated varieties have been formed. However, the storage conditions of osmanthus seeds are complex, and there are significant differences in seed vitality, this makes it difficult to identify seed viability and is not conducive to direct planting.

Similar to other agricultural and forestry crops, traditional methods for testing the vitality of osmanthus seeds include both physiological and biochemical aspects. Standard germination test [12], polymerase chain reaction [6], immunoassay test [11] and tetrazole staining method [5, 9] are often used to determine seed vigor. Although these traditional methods can be used to visually detect the vigor of seeds, these methods have many disadvantages, such as cumbersome operation, subjectivity in experiments, large environmental impacts, destructive effects on seeds, and long cycles.

In recent years, near-infrared spectroscopy, Fourier spectroscopy, and Raman spectroscopy based on optical properties have been used to identify seed vigor to distinguish, and certain research results have been obtained. For example, Song et al. demonstrated the successful put into practice of the NIR spectroscopy for non-destructive and rapid evaluation of the rice seed vitality [14]. FT-NIR spectroscopy correctly classified the active and inactive seeds of three corn seeds with an accuracy of 100% and a prediction ability of more than 95% [1]. However, these methods based on point scanning cannot get the complete information of the object.

In contrast, there are relatively few studies on detecting seed vitality of forest crops. Based on hyperspectral imaging data, the germination rates of three Australian native tree species can be accurately and non-destructively determined, with recognition ability of more than 80% [16]. It is feasible to combine hyperspectral imaging technique with Re-current neural network to predict the seed vigor of Sophora sinensis [8]. In summary, hyperspectral imaging technology has made some progress in identifying various seed vigor. However, it has not yet realized non-destructive detection of the vigor Osmanthus fragrans seeds, so this study took Osmanthus fragrans seeds with different vigor as the research object.

The specific goals this research are summarized as follows: (1) to the collect hyperspectral information of Osmanthus fragrans seeds with different varieties and vigor; (2) to compare the effects of preprocessing on PCA visualization; (3) to study the influence of pre processing and feature selection on the vigor model of the spectrum machine learning; (4) to analyze the results and advantages of CNN in the image seed vitality recognition model. The main research of this article established a vitality recognition model for osmanthus seeds from the perspectives of spectrum and image, which would provide a basis for achieving fast, accurate, and non-destructive identification of seed vitality. It also laid a theoretical foundation for the development of portable instruments that can be used for registering seeds with multiple varieties and vitality.

2. Materials and Methods

2.1. Seed Sample Preparation

Osmanthus fragrans seeds for the experiment were purchased from the Beijing seed market in September 2020, including two varieties of Jinqiugui and Rixianggui, which are referred to as JQG and RXG in this article. After bringing the seeds back to the laboratory, remove impurities and insufficient seeds. After that, the two types of seeds are divided into two

groups. One group did not do any treatment as a control group (viable seeds, with germination potential), and the other group was placed in an artificial aging box at 100°C for artificial aging, and the aging time was 12 hours (non-viable seeds, accompanied by lack of germination ability). After the aging was over and the seeds return to room temperature, 240 samples were selected from the aged and unaged seeds to start hyperspectral data collection. Finally, the germination ability of viable and inviable seeds was verified through standard germination experiments, with germination rates of 85.42% and 0, respectively.

2.2. Hyperspectral Data Acquisition and Correction

The spectrometer has a scanning range of 400-1000nm, covering visible light and part of the near-infrared region, and the spectral resolution of 4.6875nm, including 115 bands. In the processed of data acquisition, the scanning speed of the spectrometer is 30 lines, the resolution of an acquired image is 520*696. Two 150W halogen lamps (OSRAM GCA; Sylvania, Gloucester, MA, USA) were used as the light source. The distance in the hyperspectral imaging lens and sample was set to 25 cm, and the number of samples can be collected at a time was 80. Therefore, three repeated experiments were required for each type of experimental object. Part of the sample image at 727.8nm is shown in Figure 1.

Figure 1
Partial sample image at 727.8nm

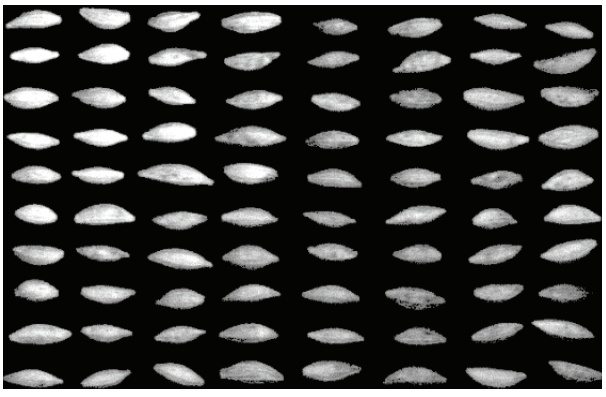

Hyperspectral data correction can eliminate the effects of different surface shapes of Osmanthus fragrans seeds, and at the same time avoid the dark current generated in the camera from interfering with hyperspectral information [10]. The specific correction formula is as follows:

$$I = \frac{I_0 - B}{W - B}, \tag{1}$$

where, I_0 represents the original hyperspectral image, and I represents the hyperspectral image after standard correction; B is the black standard reference image (obtained by completely covering the lens with an opaque cover) and W is the white standard reference image.

2.3. Spectrum and Image Information Extraction

The complete seed sample was considered an area of Interest (ROI), and then the spectrum and image information of a single seed were extracted from each ROI. After the correction of hyperspectral image, the influence of hyperspectral image background was eliminated by threshold segmentation, image filling and denoising. The image in 727.8nm band was selected as the reference, which had the largest reflectivity difference between the background and the sample area. Then, a binary image mask was created by threshold segmentation to isolate the seed region. Finally, the average spectral characteristics were calculated by averaging the intensity values of all pixels in the ROI corresponding to 115 bands of each osmanthus seed.

Due to the noise in the images corresponding to some bands at the beginning and the end, the image may not be clear. Finally, a total of 61 bands of images under 575.3-894.3nm were selected for segmentation. After the image was cropped, the image size of a single seed sample was 60*30. Some examples of individual seed samples were shown in Figure 2.

Figure 2
Some examples of hyperspectral images of Osmanthus fragrans seeds

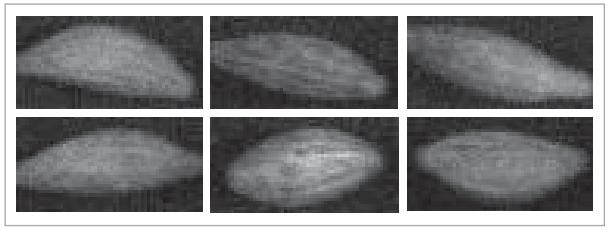

2.4. Hyperspectral Data Preprocessing

The pre-processing of hyperspectral data includes denoising and dimensionality reduction of the spectral data. In the study, multiple scattering competitive and correction adaptive weighted sampling algorithms are used to achieve spectral denoising and feature extraction, respectively. Multivariate scattering correction (MSC) [7] can effective eliminated the spectral differences caused by different scattering levels, thereby enhancing correlation in the spectrum and the data. The method corrects the baseline deviation and the deviation phenomenon of the spectral data through ideal spectrums, and separates the effective spectral information from the scattered signal through mathematical calculation, so as to eliminate the scattering effect while retaining the effective spectral information [17, 18].

The competitive adaptive Reweighted sampling (CARS) [2] uses adaptive reweighted sampling (ARS) technology to select wavelength points with large absolute value of regression coefficients. By removing the wavelength points with less weight and using interactive validation to select the subset with the smallest root-mean-square error of cross-validation (RMSECV) values, the optimal variable combination can be effectively found.

2.5. Development of Discriminant Model

Extreme Learning Machine (ELM) has the characteristics of fast learning speed and simple parameter setting, and has advantages in learning rate and generalization ability. The feedforward network neural network unit is the basic element of the standard ELM when it is constructed as a neural network. In addition to the output and input layers, the model also contains hidden layers. The output function of hidden layer is represented as:

$$f_L = \sum \beta_i h_i(x) = h(x)\beta, \tag{2}$$

where x is the input; $h(x)$ is the excitation function or feature mapping that maps the input from the original space to the feature space; β is the output weight.

K-nearest neighbor algorithm (KNN) is the simplest methods in data mining classification. All samples are classified by calculating the distance between predefined and unknown samples [13]. This similar sample splitting mode makes KNN classification algorithm more conducive to the parallel processing of large data sets, and has good classification performance for imbalanced data sets. In this paper, cross validation is used to calculate the error rate for each k classifier. Using Euclidean distance to calculate the distance between points, the formula for calculating the distance between two points (x1 and x2) in n-dimensional space is as follows:

$$d = \sqrt{\sum_{k=1}^{n} (x_1 - x_2)^2}. \tag{3}$$

CNN has the ability to assist automatic feature learning and is the efficient high-performance method for the hyperspectral data analysis. The input layer of CNN is capable of processing multidimensional data and can directly use pictures as input to the network. Therefore, in this study, the image information of osmanthus seeds with different vitality is used as input, and the two-dimensional convolutional neural network is used to realize the rapid recognition of seed vitality.

The CNN network structure diagram used in this study is shown in Figure 3. Two layers of convolution kernels were used, both of which were 5x5 in size,

Figure 3

Convolutional neural network structure diagram for seed vigor recognition

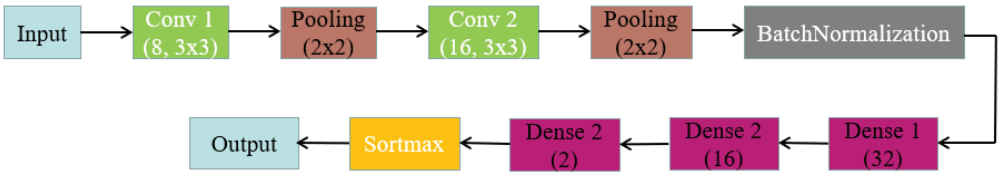

and the number of neurons in the hidden layer was 8 and 16, respectively. Using the maximum pooling method, the core size of the pooling layer was 2x2. Use Batch normation before a fully connected layer with 32 neurons, 16 neurons, and 2 neurons. It can reduce the jitter of data between different batches and increase the generalization ability to a certain extent. Finally, Softmax was used to complete the sorting of viable and non-viable Osmanthus fragrans seeds. Among them, Rectified Linear Units (ReLu) was used as the activation function. The batch size was 128, with a learning rate of 0.001, and 100 iterations per training.

3. Experimental Results

3.1. Spectral Feature Analysis

Figure 4 shows the average absorption spectra of two varieties of Osmanthus fragrans seeds (including viable and non-viable) in the 400-1000 nm spectral region. It can be seen from the figure that JQG and RXG show similar change trend even if the varieties are different. In addition, artificial aging changed the vitality of seeds, and many biochemical reactions occurred inside the seeds during this process. These reactions will change or destroy the chemical bond,

Figure 4

Average spectra of different vigor/variety seeds

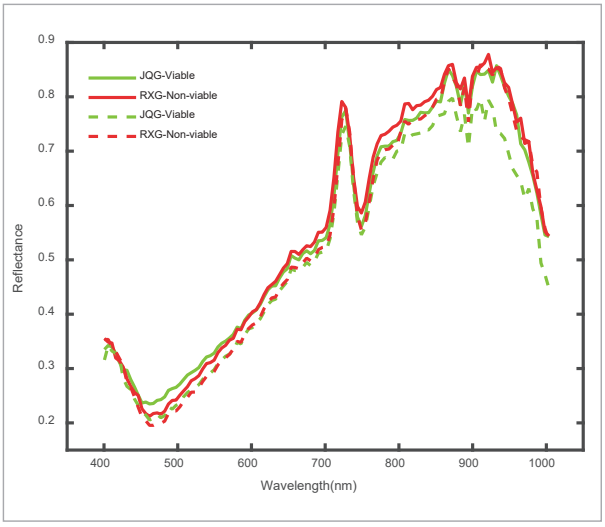

which will be reflected in the seed absorption curve. The peaks and troughs of viable seeds and non-viable seeds were in the similar positions, and they only differed in reflectivity, which was manifested in that the spectral reflectance value of non-viable seeds is lower than that of viable seeds. Peaks and valleys can reflect some information about the internal composition of the seed. For example, the absorption region near 880nm is caused by the third harmonic stretching of O-H functional group the water-related [3], and the adsorption peak near 970nm belongs to the 2nd overtone of the O-H bond [18]. Spectral research provided the qualitative analysis results for the differentiation of Osmanthus fragrans seeds with different vigor. In order to achieve accurate differentiation, further discussion is needed.

3.2. Qualitative Analysis by PCA

PCA was used to realize the clustering and visualizing the spectral data of different vigor seeds. In Figure 5, the green represents the viable seed sample, whereas the blue represents the non-viable seed sample. Figure 5(a)-(b) shows the clustering results of JQG and RXG under the original spectrum.

The contribution rates of the first three principal components are respectively given on the corresponding axis. In both JQG and RXG samples, the cumulative contribution rate of the first three principal components reached more than 85%. It can represent most information. The spectral clustering results of the surviving and non-surviving JQG seeds were very scattered and could not be effectively distinguished. Although RXG samples have obvious clustering characteristics, they cannot identify vigor well.

Therefore, MSC was used to the spectral data preprocess to reduce the influence of the noise and improve the clustering performance. Figure 5(c)-(d) shows the corresponding visualization results of the MSC pre-processing spectra. Compared with original spectral data, although there were some abnormal points, the preprocessing can enhance the clustering of the sample points and make a clear distinction in viable and non-viable seeds. The visualization of PCA further proves the practicability of using hyperspectral technology to identify seed vigor, and this result will be verified through model establishment and quantitative analysis.

Figure 5

The result graph of PCA qualitative clustering: (a) JQG+ raw spectrum; (b) RXG+ raw spectrum; (c) JQG+ MSC preprocessed spectrum; (d) RXG+ MSC preprocessed spectrum. (The green represents the viable seed sample, the blue represents the non-viable seed sample)

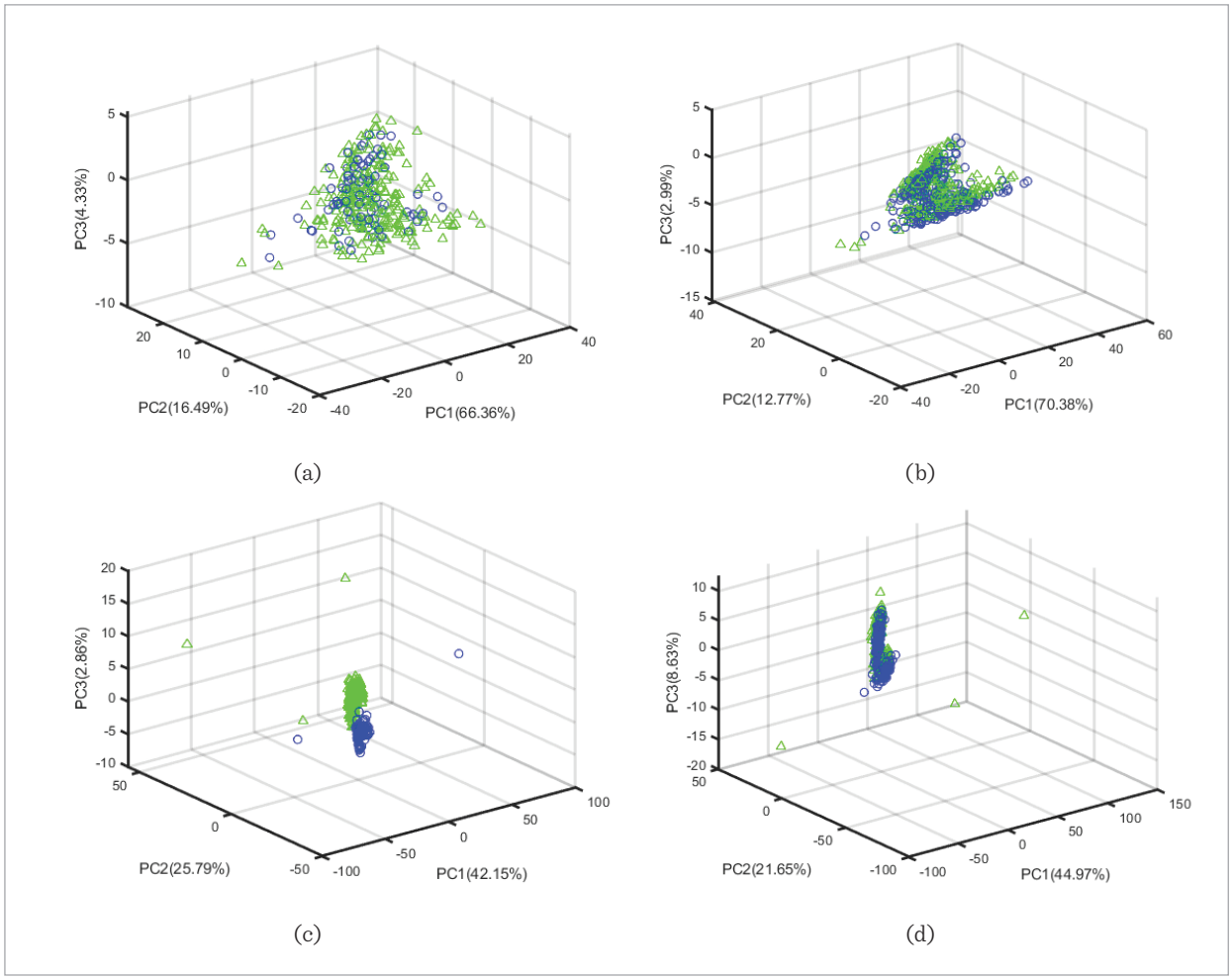

3.3. Seed Vigor Detection Model Based On Full Band

Machine learning algorithms are often combined with spectra to identify seed vigor. Therefore, this study used KNN and ELM to establish the recognition model of Osmanthus fragrans seeds with different vigor for quantitative analysis. In the model, the training and test sets are randomly divided according to 3:1, and the average of 10 runs of each model is used as the final result.

Table 1 shows the identification accuracy of seed vigor under different varieties and models. As it can see from Table 1, the accuracy of the training set is generally better than that of the test set. In the original spectrum model, JQG has a better recognition effect, and the accuracy of the test set can reach 92.5%. However, after MSC pretreatment, the ability to identify RXG seeds with different vigor was stronger. On the whole, ELM model was better than KNN model in discriminating seed vigor. Clearly, the use of MSC pretreatment methods can effectively improve the performance of the model. When MSC was combined with ELM, the recognition accuracy of JQG and RXG seeds with different vigor was 98.33% and 99.16%, respectively. The above analysis shows that the ma-

Table 1
Seed vigor recognition results based on the original spectrum

Spectral type	Model	JQG		RXG	
		Training set	Test set	Training set	Test set
Original spectrum	KNN	91.07%	81.67%	81.39%	55.83%
	ELM	98.05%	92.5%	88.33%	83.33%
MSC preprocessed spectrum	KNN	97.78%	92.5%	97.5%	96.67%
	ELM	100%	98.33%	100%	99.16%

chine learning method combined with spectral data can effectively identify different vigor of Osmanthus fragrans seeds, and the appropriate pretreatment method is an effective way to improve the accuracy.

3.4. Optimal Feature Band Selection and Extraction

When using full-band spectral data as input, there is redundant information, which affects the performance of the model competition. In order to increase the speed of analysis and modeling capabilities, one should use the adaptive weight weighted sampling algorithm (CARS) to extract the raw spectral data collection and preprocessing spectra data set on the characteristics of the wavelength. When CARS is used for feature selection, monte carlo sampling operation is set to 200 times, CARS run a total of 1000 times. By recording the run results for further analysis, we can identify the variables that give the model good generalization performance.

Figure 6 shows the process of applying CARS to select characteristic bands in the raw spectral data and preprocessed spectral datas of JQG. The number of sampling the variables decreased rapidly in first stage of the exponentially decreasing function, and then decreased very slowly in the second stage. Under different data sets, the RMSECV value showed a downward trend at the beginning of the sampling operation, and then changed in a gentle manner in the middle of the sampling operation. Finally, due to the elimination of some key variables (represented by asterisks) from the optimal subset, the information was lost, and then RMSECV grew rapidly. Therefore, the optimal subset corresponding to the lowest RMSECV value was set

Figure 6
Feature band selection using CARS: (a) JQG+ raw spectrum; (b) JQG+ MSC preprocessed spectrum

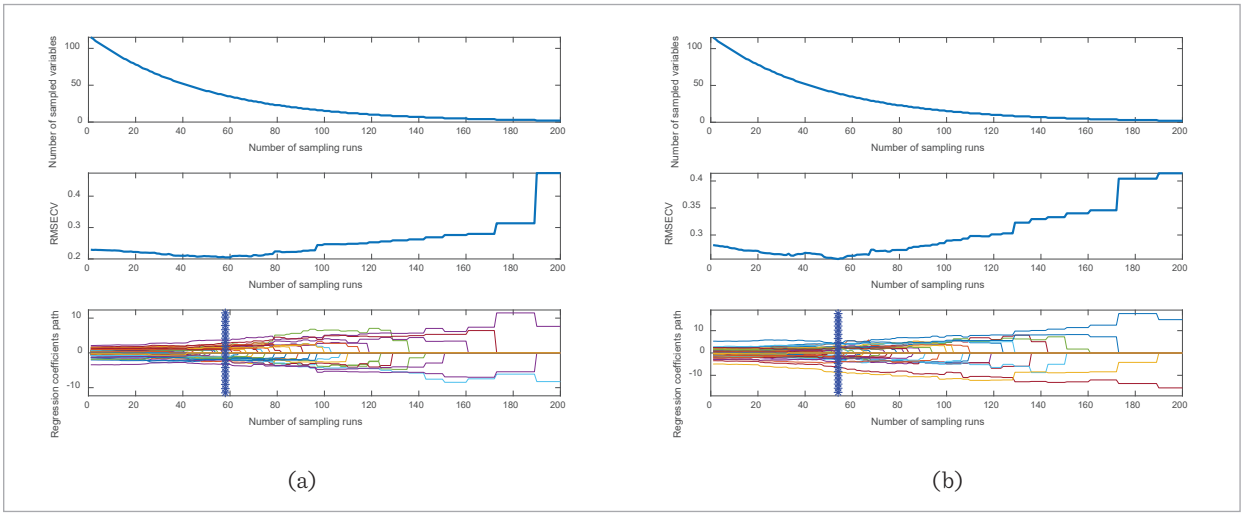

Table 2
Feature selection results under multiple spectral inputs

Spectral type	Research sample	Feature number	Wavelength (nm)
Orginal spectrum	JQG	54	436.2, 477.2, 502.9, 508.0, 518.3, 528.7, 549.4, 554.6, 559.8, 564.9, 570.1, 575.4, 580.6, 585.8, 596.2, 606.6, 611.9, 627.6, 643.3, 659.1, 664.3, 669.6, 690.7, 696.0, 706.6, 717.2, 722.5, 727.8, 733.1, 738.5, 749.1, 765.1, 770.5, 775.8, 786.5, 791.9, 797.2, 807.9, 813.3, 818.7, 824.1, 829.4, 834.8, 840.2, 861.8, 867.2, 878.1, 894.3, 910.6, 921.5, 932.4, 954.3, 970.7, 992.7
	RXG	36	461.8, 477.2, 487.4, 492.5, 497.7, 518.3, 528.7, 533.8, 564.9, 611.9, 617.1, 669.6, 690.7, 775.8, 797.2, 807.9, 813.3, 818.7, 829.5, 834.8, 845.6, 851.0, 856.4, 861.8, 872.6, 878.1, 894.3, 905.2, 910.6, 916.1, 921.5, 926.9, 932.4, 937.9, 954.3, 987.2
MSC preprocessed spectrum	JQG	42	466.8, 472.0, 502.9, 513.2, 533.8, 539.0, 570.1, 575.3, 580.5, 585.8, 590.9, 601.4, 627.6, 696.0, 701.3, 706.6, 743.8, 765.1, 781.1, 786.5, 791.9, 797.2, 802.6, 807.9, 813.3, 818.7, 824.1, 829.4, 834.8, 845.6, 851.0, 861.8, 867.2, 878.1, 888.9, 894.3, 910.6, 921.5, 932.4, 937.9, 959.7, 987.2
	RXG	39	487.4, 502.9, 523.5, 533.8, 539.0, 570.1, 575.3, 580.5, 596.2, 601.4, 627.6, 638.1, 669.6, 690.7, 696.0, 701.3, 717.2, 727.8, 743.8, 754.4, 765.1, 775.8, 786.5, 791.9, 797.2, 802.6, 807.9, 813.3,818.7, 840.2, 851.0, 861.8, 867.2, 872.6, 878.1, 894.3, 910.6, 921.5, 970.7

of optimal bands. The number of characteristic bands and specific band values extracted by CARS for different data sets are given in Table 2. They differ little in number, but differ in band distribution. The role of different band combinations will be further demonstrated by modeling.

3.5. Seed Vigor Detection Model Based on Characteristic Band

The seed viability detection models of JQG and RXG were established using the feature band data set extracted by CARS as input. The results of the training and test sets for each model are shown in Table 3. Taking the accuracy of the test set as reference, compared with the full-band model in Table 2, the accuracy of the model at this time has been improved to some extent. For both JQG and RXG's original spectral data sets, the model's improvement is not very significant, with a maximum accuracy improvement of 5%. In addition, the ELM model performs better than the KNN model with a large difference. MSC and CARS were combined to pre-process the spectral data, and the accuracy of the model was up to 100%, which showed that the different vigor of osmanthus seeds were effectively identified. Compared with the spectrum model without MSC pre-processing, the difference between the KNN and ELM models is very small, which enhances the generalization ability of the model. The above results show that the effective information in hyperspectrum can be extracted by using appropriate feature selection methods, and the model performance can be improved while the model input can be reduced.

Table 3
Identification results of seed vigor based on preprocessed spectrum

Spectral type	Model	JQG		RXG	
		Training set	Test set	Training set	Test set
Original spectrum	KNN	90.83%	80.83%	81.67%	59.17%
	ELM	97.78%	95%	93.33%	88.33%
MSC preprocessed spectrum	KNN	99.17%	100%	99.72%	100%
	ELM	100%	99.17%	100%	100%

3.6. Recognition of Seed Vigor Using Image Combined with CNN

Although spectroscopy combined with machine learning algorithms can achieve accurate identification of Osmanthus fragrans seeds with different vigor, it needs to try variety of preprocessing methods and feature selection methods to achieve the ideal model effect, and the process is cumbersome. In addtion, a two-dimensional deep learning network combined with image information collected by hyperspectral was introduced to quickly identify seed vigor. Modeling and analysis were also carried out for the full-band image and the feature-band image extracted by CARS. When training model, training set and testing set are random divided according to the proportion of 3:1.

Table 4 shows the performance of each model, including the belt and the discriminant result of each model. It can be seen that in the image model, the accuracy and loss functions of the training set and the test set show a high degree of consistency. Compared to the spectrum-machine learning model, the image-deep learning model has better recognition performance for different vitality seeds. In both full band and characteristic band models, the accuracy was close to 100%, and the loss function was close to 0. Moreover, the ability to recognize different vigorous JQG seeds and RXG seeds was equivalent, which proves that the model had a stronger generalization function. In summary, when identifying Osmanthus fragrans seeds with different vigor, Deep learning approach can effectively extract the image characteristics of deep make the model more accurate.

Table 4
Model performance of seed vigor discrimination based on image information combined with CNN

Model input	JQG				RXG			
	Training set		Test set		Training set		Test set	
	Acc	Loss	Acc	Loss	Acc	Loss	Acc	Loss
ALL (61)	100%	5.4e-6	99.85%	0.0046	100%	7.3e-6	99.88%	0.0034
CARS (37)	100%	5.3e-6	99.91%	0.002	100%	6.4e-6	99.55%	0.0152

4. Conclusions

This article highlights music-like technology combined with a variety of machine learning and deep learning algorithms to identify the living and non-living Osmanthus flower seeds of two varieties. The spectral changes of different varieties of Osmanthus seeds were similar, and the average spectral reflectance of active seeds was higher than that of inactive seeds. Through the visual analysis of PCA+MSC, the qualitative differentiation of seeds with different vigor was realized. ELM performs better than KNN in spectrum machine learning models. Moreover, the ability to recognize JQG was better, but the overall accuracy of original spectral model was lower. The application of the MSC and CARS can achieve higher accurate recognition with less input, and the model accuracy rate was close to 100%. Different from machine learning model, depth model with image as input can achieve good recognition effect without complex preprocessing. It can be seen that both spectral information and image information can play a key role in identifying seed vigor. This study shows that it is feasible to use hyperspectral imaging to identify different varieties and vigour of osmanthus seeds. In addition, the proposed approach of spectrum traditional machine learning and image deep learning can enhance the recognition ability of hyperspectral information through the combination of different features and multiple algorithms. In subsequent research, more algorithms can be used as an attempt to distinguish seeds of different vitality and varieties, thereby increasing the generalization adaptability and ability of the model and facilitating the development of portable instruments.

Acknowledgements

This work was partly supported by the 2021 the ordinary university key research platform and projects of GuangDong: The uncontrolled environment oriented pedestrians to identify key technology research (Grant: 2021ZDZX1047), and in part by the 2020 Guangdong University of Science and Technology School-level Innovation and Strong School Project: Comprehensive Data Management and Application Research Center (Grant: GKY-2020CQJG-1), and in part by Guangzhou Science and Technology Project under Grant No.202102080656 and No.202002030273.

References

1. Ambrose, A., Lohumi, S., Lee, W-H., Cho, B K. Comparative Nondestructive Measurement of Corn Seed Viability Using Fourier Transform Near-Infrared (FT-NIR) and Raman Spectros-copy. Sensors and Actuators B: Chemical, 2016, 224, 500-506. https://doi.org/10.1016/j.snb.2015.10.082
2. Chu, Y. W., Tang, S. S., Ma, S. X., Yu, Y. M., Zhong, Q. H., Yang, M. G., Lian, B. G., Yong, F L., Xiao, Y. Z. Accuracy and Stability Im-provement for Meat Species Identification Us-ing Multiplicative Scatter Correction and La-ser-Induced Breakdown Spectroscopy. Optics Express, 2018, 26, 10119-10127. https://doi.org/10.1364/OE.26.010119
3. Chen, L. C., Papandreou, G., Kokkinos, L., Murphy, K., Yuille, A. L. DeepLab: Semantic Image Segmentation with Deep Convolutional Nets, Atrous Convolution, and Fully Connected CRFs. IEEE Transactions on Pattern Analysis and Machine Intelligence, 2018, 40, 834-848. https://doi.org/10.1109/TPAMI.2017.2699184
4. Grasso, R., Gulino, M., Giuffffrid, F., Agnello, M., Musumeci, F., Scordino, A. Non-Destructive Evaluation of Watermelon Seeds Germination by Using Delayed Lumi-nescence. Journal of Photochemistry and Pho-tobiology B-Biology, 2018, 187, 126-130. https://doi.org/10.1016/j.jphotobiol.2018.08.012
5. Hosomi, S. T., Custódio, C. C., Seaton, P. T., Marks, T. R., Machado-Neto, N. B. Improved Assessment of Viability and Germination of Cattleya (Orchidaceae) Seeds Following Stor-age. In Vitro Cellular and Developmental Biol-ogy Plant, 2012, 48, 127-136. https://doi.org/10.1007/s11627-011-9404-1
6. Izabel, C. S. N., Von Pinho, É. V. D. R., Viviane, M. D. A., Heloisa, O. D. S., Danielle, R. V., Ren-zo, G. V. P., Maria, L. M. C. Enzyme Activities and Gene Expression in Dry Maize Seeds and Seeds Submitted to Low Germination Temper-ature. African Journal of Agricultural Research, 2016, 11, 3097-3103. https://doi.org/10.5897/AJAR2016.11115
7. Mo, C., Kim, K., Lee, K., Kim, M. S., Cho, B. K., Lim, K., Kang, S. Nondestructive Quality Eval-uation of Pepper (Capsicum annuum L.) Seeds Using LED-Induced Hyperspectral Reflectance Imaging. Sensors, 2014, 14 (4), 7489-7504. https://doi.org/10.3390/s140407489
8. Nansen, C., Zhao, G., Dakin, N., Zhao, C., Turner, S. R. Using Hyperspectral Imaging to Determine Germination of Native Australian Plant Seeds. Journal of Photochemistry and Photobiology B: Biology, 2015, 145, 19-24. https://doi.org/10.1016/j.jphotobiol.2015.02.015
9. Olesen, M H., Nikneshan, P., Shrestha, S., Tadayyon, A. Viability Prediction of Ricinus cummunis L. Seeds Using Multispectral Imag-ing. Sensors, 2015, 15, 4592-4604. https://doi.org/10.3390/s150204592
10. Pang, L., Wang, L., Yuan, P., Yan, L., Xiao, J. Rapid Seed Viability Prediction of Sophora Ja-ponica by Improved Successive Projection Al-gorithm and Hyperspectral Imaging. Infrared Physics and Technology, 2022, 123, 104143. https://doi.org/10.1016/j.infrared.2022.104143
11. Rahman, A., Cho, B. K. Assessment of Seed Quality Using Non-Destructive Measurement Techniques: A Review. Seed Science Research, 2016, 26, 285-305. https://doi.org/10.1017/S0960258516000234
12. Shrestha, S., Knapič, M., Žibrat, U., Deleuran, L C., Gislum, R. Single Seed Near-Infrared Hy-perspectral Imaging in Determining Tomato (Solanum lycopersicum L.) Seed Quality in As-sociation with Multivariate Data Analysis. Sensors and Actuators B: Chemical, 2016, 237, 1027-1034. https://doi.org/10.1016/j.snb.2016.08.170
13. Song, L., Wang, Q., Wang, C., Lin, Y., Yu, D., Xu, Z., Huang, Q., Wu, Y. Effect of Gam-ma-Irradiation on Rice Seed Vigor Assessed by Near-Infrared Spectroscopy. Journal of Stored Products Research, 2015, 62, 46-51. https://doi.org/10.1016/j.jspr.2015.03.009

14. Wang, Z X., Zhang, R. The Complete Mito-chondrial Genome of Osmanthus Fragrans (Lamiales, Oleaceae) from China. Mitochon-drial DNA Part B, 2021, 6(7), 2056-2057. https://doi.org/10.1080/23802359.2021.1942265

15. Wakholi, C., Kandpal, L. M., Lee, H., Bae, H., Park, E., Kim, S. M., Mo, C., Lee, W.-H., Cho, B.-K. Rapid Assessment of Corn Seed Viability Using Short Wave Infrared Line-Scan Hyper-spectral Imaging and Chemometrics. Sensors and Actuators B: Chemical, 2018, 255, 4098-507. https://doi.org/10.1016/j.snb.2017.08.036

16. Weng, S., Tang, P., Yuan, H., Guo, B., Yu, S., Huang, L., Xu, C. Hyperspectral Imaging for Accurate Determination of Rice Variety Using a Deep Learning Network with Multi-Feature Fusion. Spectrochimica Acta Part A: Molecular and Biomolecular Spectroscopy, 2020, 234, 118237. https://doi.org/10.1016/j.saa.2020.118237

17. Zhang, X., Liu, F., He, Y., Gong, X. Detecting Macronutrients Content and Distribution in Oilseed Rape Leaves Based on Hyperspectral Imaging. Biosystems Engineering, 2013, 115, 56-65. https://doi.org/10.1016/j.biosystemseng.2013.02.007